

## ON SPHERICAL CR UNIFORMIZATION OF 3-MANIFOLDS

MARTIN DERAUX

ABSTRACT. We consider the discrete representations of 3-manifold groups into  $PU(2, 1)$  that appear in the Falbel-Koseleff-Rouillier, such that the peripheral subgroups have cyclic unipotent holonomy. We show that two of these representations have conjugate images, even though they represent different 3-manifold groups. This illustrates the fact that a discrete representation  $\pi_1(M) \rightarrow PU(2, 1)$  with cyclic unipotent boundary holonomy is not in general the holonomy of a spherical CR uniformization of  $M$ .

## 1. INTRODUCTION

It is a difficult problem to characterize 3-manifolds which admit a spherical CR uniformization, i.e. manifolds which can occur as the manifold at infinity of some infinite volume complex hyperbolic surface (or perhaps complex hyperbolic orbifold with isolated singularities).

Of course  $S^3$  as well as lens spaces trivially admit a spherical CR uniformizations (the orbifold fundamental group of the corresponding complex hyperbolic quotient is then a finite cyclic group). Quotients of the 3-dimensional Heisenberg group by lattices also provide another somewhat trivial class, since once can think of the Heisenberg group as a model of  $\partial H_{\mathbb{C}}^2 \setminus \{pt\}$ ; this class consists of circle bundles over a 2-torus. More generally, it is well known that many Seifert fibrations occur, by taking deformations of Fuchsian subgroups of  $PU(2, 1)$ . For small deformations, the corresponding quotients are disk bundles over surfaces (or more generally 2-dimensional orbifolds), yielding circle bundles as manifolds at infinity. Note that none of the above examples are hyperbolic manifolds.

In the last decade, R. Schwartz discovered that many hyperbolic manifolds can occur as well, see [31] for a nice overview of his constructions. The starting point was the construction of a spherical CR uniformization of the Whitehead link complement [28], and of a *closed* hyperbolic 3-manifold [30]. Schwartz went on to produce infinitely many examples through a somewhat delicate Dehn surgery theorem. Recent work of Parker and Will [24] shows that the Whitehead link complement admits at least two distinct spherical CR uniformizations, i.e. it occurs as the manifold at infinity of two non-isometric complex hyperbolic orbifolds.

The figure eight knot complement was shown to admit a spherical CR uniformization [8]. In fact it turns out uncountably many pairwise non-conjugate discrete subgroups of  $PU(2, 1)$  yield the figure eight knot as their manifold at infinity, see [7].

The general question of the classification of hyperbolic 3-manifolds which admit a spherical CR uniformization is still widely open.

A general approach to investigate the above general question was laid down by Falbel a few years ago. He devised a computational way to determine all the conjugacy classes of representations of the fundamental group of any given open 3-manifolds (with torus ends) with unipotent boundary holonomy. The rough idea is to use an ideal triangulation of the manifold, so that representations are parametrized by cross-ratios of quadruples of points in  $\partial_\infty H_{\mathbb{C}}^2$ , and to write compatibility equations for these cross-ratios to yield a representation (with appropriate boundary holonomy conditions). For more information on this, see [11], [2] and for another parametrization of the representation variety, see [15].

For manifolds that can be built by gluing up to three tetrahedra, the solutions to the compatibility equations can be computed using current computer technology (and somewhat sophisticated computational techniques for solving polynomial systems), see [12]. We will refer to this list of representations as the FKR census.

It turns out there are in fact very few discrete representations in the FKR census. Since the representations in the census are not representative of the whole character variety (for computational convenience, the authors list only representations where the peripheral holonomy consists of unipotent matrices), we will not take the trouble of giving detailed arguments that prove non-discreteness results.

We focus on cases where we know the representation is discrete, namely the pairs  $(M, \rho)$  in Table 1. We suspect that these are in fact the only discrete representations into  $PU(2, 1)$

- (1) m003,  $\rho = \rho_{2,1}$
- (2) m004,  $\rho = \rho_{1,1}$
- (3) m004,  $\rho = \rho_{3,1}$
- (4) m004,  $\rho = \rho_{4,1}$
- (5) m009,  $\rho = \rho_{4,3}$
- (6) m015,  $\rho = \rho_{3,3}$

TABLE 1. The list of discrete representations in the FKR census, for non-compact manifolds built out of at most three tetrahedra.

in the FKR census (apart from the representations with finite image, which do not appear in the list in [12]).

Note that it is not clear whether discreteness of a representation  $\rho : \pi_1(M) \rightarrow PU(2, 1)$  (even together with boundary parabolicity) suffices to guarantee that  $\rho$  is the holonomy of a spherical CR structure on  $M$ . The main problem is that there is no natural way to extend quadruples of points to full-fledged tetrahedra in  $\partial H_{\mathbb{C}}^2$ . For instance, the attempts in [11] and [13] yield branched CR structures, and it is not known whether these representations are the holonomy of an unbranched CR structure.

In fact we will be more restrictive and require not only that  $\rho$  be the holonomy of a structure, but that it produce a spherical CR **uniformization** of  $M$  (Schwartz call these *complete* spherical CR structures, see [31] for instance). We briefly recall basic definitions pertaining to this notion.

Recall that a discrete group  $\Gamma \subset PU(2, 1)$ , acts properly on the complex hyperbolic plane  $\mathbf{H}_{\mathbb{C}}^2$ . The action extends to its boundary at infinity  $\partial_{\infty} \mathbf{H}_{\mathbb{C}}^2$ , but it is usually no longer proper.

**Definition 1.1.** *The domain of discontinuity  $\Omega_{\Gamma}$  is the largest open subset of  $\partial_{\infty} \mathbf{H}_{\mathbb{C}}^2$  where the action is proper. Its complement  $\Lambda_{\Gamma} = \partial_{\infty} \mathbf{H}_{\mathbb{C}}^2 - \Omega_{\Gamma}$  is called the limit set of  $\Gamma$ .*

When the action of  $\Gamma$  on  $\Omega_{\Gamma}$  has no fixed points, the quotient  $\Gamma \backslash \Omega_{\Gamma}$  is a manifold, which of course carries a CR structure inherited from the standard CR structure on  $\partial_{\infty} \mathbf{H}_{\mathbb{C}}^2 \simeq S^3$ .

**Definition 1.2.** *Let  $\Gamma \subset PU(2, 1)$  be a discrete group whose action on  $\mathbf{H}_{\mathbb{C}}^2$  has only isolated fixed points. Then the quotient  $\Gamma \backslash \Omega_{\Gamma}$  is called the **manifold at infinity** of  $\Gamma$ .*

We will sometimes call  $\Gamma \backslash \Omega_{\Gamma}$  the manifold at infinity of  $\Gamma$ , rather than the manifold at infinity of  $\Gamma \backslash H_{\mathbb{C}}^2$ .

**Definition 1.3.** *Let  $\rho : \pi_1(M) \rightarrow PU(2, 1)$  be a representation. We say that  $\rho$  gives a spherical CR uniformization of  $M$  if  $\Gamma = \text{Im}(\rho)$  is discrete, all its fixed points in  $\mathbf{H}_{\mathbb{C}}^2$  are isolated, and the manifold at infinity of  $\Gamma$  is homeomorphic to  $M$ .*

We now summarize what is known about the representations that appear in Table 1, in historical order (the numbers opening each paragraph are given to follow the notation in the table).

(2), (3), (4) The representations of  $\pi_1(\mathfrak{m}004)$  were studied in [11] and [8]. They are all discrete, non-faithful representations.

(3) The group  $\text{Im}(\rho_{3,1})$  can be checked to be a (non-elementary) normal subgroup of the Eisenstein-Picard lattice, i.e. a normal subgroup of  $PU(2, 1, \mathbb{Z}[\omega])$  (see [11]). It follows that its limit set is all of  $S^3$ , or equivalently that it has empty domain of discontinuity. This makes it obvious that  $\rho_{2,1}$  is not the holonomy of a uniformization (but it is not known whether it is the holonomy of a spherical CR structure).

(1) A similar property holds for the image  $\text{Im}(\rho_{2,1})$  of the only representation of  $\pi_1(\mathfrak{m}003)$  in the FKR census, which is a normal subgroup of a lattice sometimes referred to as the sister of the Eisenstein-Picard lattice (the Eisenstein-Picard lattice and its sister have the same covolume, and up to conjugation they are the only non-uniform arithmetic lattices with that volume, see [32]).

(2), (4) The two other representations of  $\pi_1(\mathfrak{m}004)$  were studied in [8], where the author and Falbel gave a proof that they both give a spherical CR uniformization of the figure eight knot complement (in fact these two representations differ by precomposition by an orientation reversing outer automorphism of  $\pi_1(\mathfrak{m}004)$ ).

A more enlightening fundamental domain for the action of the group  $\text{Im}(\rho_{1,1})$  can be obtained quite naturally as a Ford domain centered at the fixed point of the image of a peripheral subgroup, as worked out in [7]. That domain exhibits an explicit horotube structure for the group, as defined in [31]. Moreover, the combinatorial structure of the Ford fundamental domain exhibits striking similarities with the structure of the Ford domain in  $H_{\mathbb{R}}^3$  for the holonomy group of the unique complete hyperbolic structure on the figure eight knot complement.

(5) Performing the same analysis for other discrete groups with cyclic unipotent holonomy in the FKR census, one gets the following:

**Theorem 1.4.** *The representation  $\rho_{4,3}$  is the holonomy of a spherical CR uniformization of  $M = \mathfrak{m}009$ .*

Rather than using the group of the FKR census, we will give a triangle group interpretation of that group, in the spirit of Schwartz's constructions. This will make it easier for the reader to get explicit matrices for the group.

The author went through the same analysis as in [7] and worked out the combinatorics of the Ford domain for  $Im(\rho_{4,3})$  (really, he instructed the computer to work this out for him). The group presentation then comes for free from the Ford domain. From that Ford domain, it is relatively easy to compute the fundamental group of the manifold at infinity, and to find an explicit isomorphism with the fundamental group of  $\mathfrak{m}009$  (of course one also needs to check that the peripheral subgroups correspond in this isomorphism).

The details are quite unpleasant to write in a paper (see [7] for similar arguments), so we will not give the details of the proof of Theorem 1.4. We only focus on proving discreteness and getting a group presentation for  $Im(\rho_{4,3})$  (see Theorem 5.3).

Note that, unlike the case of the figure eight knot complement, the boundary of the complex hyperbolic Ford domain does not have exactly the same local combinatorial structure as the Ford domain of the real hyperbolic structure (compare the 2-faces of Figure 1 with the shaded 2-faces in Figures 2, 3).

(5)=(6) In view of the main results of [30], [8] and Theorem 1.4, one may be tempted to dream of a positive answer to the following question raised by Falbel:

**Question:** Let  $M$  be a non-compact hyperbolic 3-manifold of finite volume, and let  $\rho : \pi_1(M) \rightarrow PU(2, 1)$  be a *discrete* representation such that every peripheral subgroup is mapped to a cyclic group generated by a unipotent element. Is the manifold at infinity of  $\rho(\pi_1(M))$  homeomorphic to  $M$ ?

The requirement that peripheral  $\mathbb{Z} \oplus \mathbb{Z}$  subgroups are mapped to subgroups isomorphic to  $\mathbb{Z}$  is included because of the results in [11] (the corresponding representation is boundary injective, but the domain of discontinuity is empty, so there is no manifold at infinity at all).

The next result shows that the answer is negative in general; it suggests one needs to be very cautious when studying representations of 3-manifolds into  $PU(2, 1)$ .

**Theorem 1.5.** *The groups  $\rho_{3,3}(\pi_1(\mathfrak{m}015))$  and  $\rho_{4,3}(\pi_1(\mathfrak{m}009))$  are conjugate in  $PU(2, 1)$ .*

In section 5, we will prove that both representations are discrete, have non-empty domain of discontinuity, and that the image group has only isolated fixed points in  $\mathbf{H}_{\mathbb{C}}^2$ . In particular at least one of the two manifolds gives a negative answer to Falbel's question. Using Theorem 1.4 (which we will not prove), one would see that the negative answer is actually provided by the manifold  $\mathfrak{m}015$ . In other words, the manifold at infinity of  $\rho_{3,3}(\pi_1(\mathfrak{m}015))$  is *the wrong manifold*, in the sense that it is homeomorphic to  $\mathfrak{m}009$ , *not* to  $\mathfrak{m}015$ .

Let us emphasize once more that Theorem 1.5 shows that a discrete, boundary unipotent representation of the fundamental group of a given non-compact manifold into  $PU(2, 1)$ , is not necessarily the holonomy of a spherical CR uniformization of that manifold, even if the peripheral holonomy is cyclic.

In section 3 we will describe a technical feature shared by all the noncompact hyperbolic manifolds that are known to admit a spherical CR uniformization. For the time being, this feature may serve as an explanation for the existence of these exotic uniformizations. Specifically, it turns out that all finite volume non compact 3-manifolds that are known to admit a spherical CR uniformization all admit an exceptional Dehn filling that is a Seifert fibration over a  $p, q, r$ -orbifold (see Theorem 3.1) with  $p, q, r \geq 3$ . For 3-manifolds that do not have such Seifert Dehn fillings, no satisfactory evidence of non-existence of spherical CR uniformizations is presently available (but the FKR census gives no discrete representation with cyclic unipotent boundary holonomy).

Now theorem 1.5 will be an obvious consequence of a stronger statement, namely Theorem 4.2, which gives a way to reconstruct the image of the two relevant FKR census representations directly by deforming triangle groups. The idea is to take the obvious embedding of the 3,3,5-triangle group, obtained via the injection  $SO(2, 1) \subset SU(2, 1)$ , where reflections in  $H_{\mathbb{R}}^2$  are extended to complex reflections in  $H_{\mathbb{C}}^2$ . Note that this representation is type-preserving, in the sense that elliptic (resp. parabolic, loxodromic) elements are mapped to elliptic (resp. parabolic, loxodromic) elements.

The index two subgroup of words of even length in the triangle group has a manifold at infinity which is a Seifert fibration over the 3,3,5-orbifold (see chapter 4 of [31]). It is well known that, modulo conjugation in  $PU(2, 1)$ , the deformation space of this representation of the 3,3,5-triangle group is an interval (see [29] for instance), and one expects that, at least for small deformations, the group should remain discrete, and the manifold at infinity should not change its homeomorphism type.

The idea is then to consider the first place in the deformation space where the representation is no longer type-preserving. A conjectural quantitative analysis of when this happens is stated in [29]; in the case at hand, the first change in types should occur when the word  $I_2 I_3 I_1 I_3$  (which is loxodromic in the original triangle group) becomes parabolic. We will call the corresponding group the first 3,3,5-triangle group with an *accidental parabolic element*, even though the validity of this description really relies on the validity of Schwartz's conjectures. This group is often denoted  $(3, 3, 5; \infty)$  in the literature.

In this paper, we describe explicit representations of  $\pi_1(\mathbf{m009})$  and  $\pi_1(\mathbf{m015})$  onto the  $(3, 3, 5; \infty)$  triangle group, and show that they map peripheral subgroups to cyclic subgroups generated by the accidental parabolic element. The accidental parabolic element is a unipotent element, i.e. it has 1 as its only eigenvalue (see section 3). From this one can easily identify these two representations as specific representations in the FKR census (see section 4).

We finish by noting that the result of Theorem 4.2, even though it gives a way to bypass the use of the FKR census, was widely inspired by detailed inspection of the representations in the census. Originally, the author had computed Ford domains for the image of the

census representations that looked discrete, and noticed that two of these Ford domains were isometric.

In that sense, the Ford domain of a group (centered at the fixed a suitably chosen parabolic element) gives a very efficient conjugacy invariant of the group, just like it does in the real hyperbolic case (in that case, the tiling dual to the tiling by the Ford domain produces the so-called canonical decomposition, see [10]).

**Acknowledgements:** This work was partly supported by the ANR, through the grant SGT (“Structures Géométriques Triangulées”). The author also benefited from generous support from the GEAR network (NSF grants DMS 1107452, 1107263, 1107367), via funding of an long term visit at ICERM; the author warmly thanks ICERM for its hospitality, Elisha Falbel, Pierre-Vincent Koseleff and Fabrice Rouillier for sending him an early version of their census; Ben Burton, Nathan Dunfield and Dave Futer for useful conversations related to this work; and finally the referee, who suggested several improvements in the manuscript.

## 2. FORD DOMAINS IN $H_{\mathbb{R}}^3$

We briefly recall the general notion of Ford domain for discrete subgroups of  $PSL_2(\mathbb{C}) = Isom(H_{\mathbb{R}}^3)$ , and describe these domains for the special case of the holonomy group of the complete hyperbolic structures on three specific 3-manifolds, namely **m004**, **m009**, **m015** in the Hildebrand-Weeks census.

**2.1. Real hyperbolic space and Ford domains.** Here we view  $H_{\mathbb{R}}^3$  as the upper half space

$$\{(z, t) \in \mathbb{C} \times \mathbb{R} : t > 0\},$$

with the metric  $(dx^2 + dy^2 + dt^2)/t^2$ . Recall that  $\Gamma \subset PSL_2(\mathbb{C})$  acts on  $\partial_{\infty} H_{\mathbb{R}}^3 \simeq P_{\mathbb{C}}^1$  by its linear action on  $C^2$ . Working in an affine chart, one gets an action by fractional linear transformations, i.e.

$$z \mapsto \frac{az + b}{cz + d}.$$

The basic point is that these maps extend to give an isometric action of  $PSL_2(\mathbb{C})$  on  $H_{\mathbb{R}}^3$ , uniquely determined by the fact that circles in  $\mathbb{C}$  give the boundary of a unique sphere in  $\mathbb{C} \times \mathbb{R}$  orthogonal to the horizontal plane  $\mathbb{C}$ .

A formula for the extension can be most easily obtained by seeing  $H_{\mathbb{R}}^3$  as a totally geodesic subspace of  $H_{\mathbb{H}}^4$ , which is isometric to  $H_{\mathbb{H}}^1$ , the 1-dimensional quaternionic hyperbolic space, see [22] for instance. Concretely, one gets

$$(z, t) \mapsto \left( \frac{(az + b)(\bar{c}\bar{z} + \bar{d}) + a\bar{c}t^2}{|cz + d|^2 + |c|^2t^2}, \frac{t}{|cz + d|^2 + |c|^2t^2} \right).$$

Now let

$$\gamma = \begin{pmatrix} a & b \\ c & d \end{pmatrix},$$

and suppose  $c \neq 0$ , or equivalently that  $\gamma$  does not fix infinity.



**Definition 2.1.** *The isometric circle of  $\gamma$  is the circle in  $\mathbb{C}$  where the derivative of the corresponding fractional linear transformation has modulus 1, which has equation  $|cz + d| = 1$ . The isometric sphere of  $\gamma$  is the unique sphere in  $\mathbb{C} \times \mathbb{R}$  orthogonal to  $\mathbb{C}$  that contains its isometric circle, with equation  $|cz + d|^2 + |tc|^2 = 1$ .*

Note that the circle has center  $-d/c$  and radius  $1/|c|$ . Moreover, it is easy to see that  $\gamma$  maps its isometric circle to the isometric circle of  $\gamma^{-1}$ . Finally, note that the hemispheres in  $\mathbb{C} \times \mathbb{R}$  orthogonal to  $\mathbb{C}$  are totally geodesic copies of  $H_{\mathbb{R}}^2$  in  $H_{\mathbb{R}}^3$ .

**Definition 2.2.** *The Ford domain of  $\Gamma$  in  $\mathbb{H}_{\mathbb{R}}^3$  is the connected component containing infinity of the complement of all isometric spheres of elements in  $\Gamma$ .*

Provided the group  $\Gamma$  is discrete, its Ford domain is a fundamental domain for the action of  $\Gamma$  if and only if no element of  $\Gamma$  fixed infinity. It is useful to normalize the matrices so that infinity does have a nontrivial stabilizer, in which case the stabilizer acts on  $\mathbb{C} \simeq \partial_{\infty} H_{\mathbb{R}}^3$  by a group  $S$  of similarities, and one gets a fundamental domain for the decomposition of  $\Gamma$  into  $S$ -cosets (see [1] for instance).

**2.2. The Hildebrand-Weeks census.** The Hildebrand-Weeks census is a list of all 1-cusped hyperbolic 3-manifolds that can be built by gluing up to 5 tetrahedra, see [19]. For completeness, we mention that the census was subsequently extended to allow for more tetrahedra, see [5], see also the work of Thistlethwaite [33], and Burton [4], but the manifolds we consider in this paper require only 3 ideal tetrahedra.

Recall that when it exists, the complete hyperbolic metric actually has finite volume, so the metric is unique by Mostow rigidity; in other words, the Kleinian groups are determined *up to conjugation* in  $PSL_2(\mathbb{C})$ . Because of the issue of possible conjugation, it is sometimes difficult to compare different groups, but there is a canonical way to associate a triangulation, obtained by taking the decomposition *dual* to the Ford domain (see [10]).

This canonical decomposition is of course encoded in SnapPy; we will start our description from the output of SnapPy for each of the three manifolds considered in this paper, obtained with the `canonicalize` command (we are using SnapPy version 2.0, but the commands we use are so standard that they should remain stable in subsequent versions). In order to avoid cumbersome notation, throughout section 2, we will use the same notation for generators in group presentations, and their image in  $PSL_2(\mathbb{C})$ , so  $x$  will sometimes stand for  $\rho(x)$ ; this is reasonable because all the representations we consider in this section are known to be faithful.

### 2.2.1. m004. Presentation:

$$\langle x, y \mid x[x, y][y^{-1}, x^{-1}] \rangle$$

**Generators of a peripheral subgroup:**

$$xy, \quad [x, y^{-1}][x^{-1}, y^{-1}]$$

**Shape of the cusp:**

$$2i\sqrt{3}$$

**Triangular generators:**

$$x^2yx^{-1} = \begin{pmatrix} 1 & 0 \\ \alpha & 1 \end{pmatrix}, \quad xyx = \begin{pmatrix} 1 & \alpha \\ 0 & 1 \end{pmatrix},$$

where  $\alpha = \frac{i-\sqrt{3}}{2}$ , which has minimal polynomial  $x^4 - x^2 + 1$ . Note that there is in fact a representation into  $PSL_2(K)$  for a smaller number field, but we will not need this here.

The triangular shape of  $s = x^2yx^{-1}$  and  $t = xyx$  is easy to guess from the SnapPy canonical presentation; it is not completely obvious that these two matrices generate the whole group, so we mention that

$$[s^{-1}, t] = x[y^{-1}, x^{-1}]x^2yx^{-2}y^{-1}x^{-1} = x[y, x]xyx^{-2}y^{-1}x^{-1} = xyt^{-1},$$

so  $xy$  is in the group generated by  $s$  and  $t$ , which easily proves that  $s$  and  $t$  generate.

Finally, we summarize how to obtain the minimal polynomial of  $\alpha$ . Using  $s$  and  $t$  as generators, the previous discussion implies

$$x = \begin{pmatrix} -\alpha^2 + 1 & -\alpha^3 \\ \alpha^3 & \alpha^4 + \alpha^2 + 1 \end{pmatrix}, \quad y = \begin{pmatrix} \alpha^4 + 2\alpha^2 + 1 & 2\alpha^3 + \alpha \\ -2\alpha^3 & -2\alpha^2 + 1 \end{pmatrix}.$$

The relation in the presentation translates into a set of polynomial equations in  $\alpha$ . Specifically, we require that  $M = x[x, y][y^{-1}, x^{-1}]$  is scalar, which becomes

$$\begin{aligned} M_{1,2} &= -\alpha^3(\alpha^4 + \alpha^2 + 1)(\alpha^4 - \alpha^2 + 1)(\alpha^8 - \alpha^4 + 2\alpha^2 + 1) = 0 \\ M_{2,1} &= \alpha^3(\alpha^4 + \alpha^2 + 1)^2(\alpha^4 - \alpha^2 + 1)^2 = 0 \\ M_{1,1} - M_{2,2} &= -\alpha^2(\alpha^4 + \alpha^2 + 1)(\alpha^4 - \alpha^2 + 1)(\alpha^{10} + 2\alpha^8 - \alpha^6 + 2\alpha^4 + \alpha^2 + 2) = 0 \end{aligned},$$

so taking  $\alpha$  to be a root of  $x^4 - x^2 + 1$  will certainly give a representation into  $PSL_2(\mathbb{C})$  (other choices of  $\alpha$  will give Galois conjugate representations).

In particular, for  $\alpha = (i - \sqrt{3})/2$ , one gets lower triangular matrices for the stabilizer of a cusp by computing

$$x^2yx^{-1} = \begin{pmatrix} 1 & 0 \\ \alpha & 1 \end{pmatrix}, \quad x[x, y][x, y^{-1}]x^{-1} = \begin{pmatrix} -1 & 0 \\ -\sqrt{3} - 3i & -1 \end{pmatrix}.$$

and the ratio of the lower left entries give the shape of the cusp, namely

$$-\frac{\sqrt{3} + 3i}{\alpha} = 2i\sqrt{3}.$$

**2.2.2. m009. Presentation:**

$$\langle x, y \mid x[x, y]x[x, y^{-1}] \rangle$$

**Generators of a peripheral subgroup:**

$$xy, \quad x^{-1}y^{-1}x^3y^{-1}x^{-1}y$$

**Shape of the cusp:**

$$i\sqrt{7}$$



The SnapPy representations give matrices with entries in  $\mathbb{Q}(i, \beta)$ , where

$$\beta^4 + \beta^2 + 2 = 0.$$

The specific matrices are then given by

$$x = \begin{pmatrix} -\beta^3 - \beta & i \\ -i & \beta \end{pmatrix}, \quad y = \begin{pmatrix} -\beta^3 & i \\ -i(\beta^2 + 1) & \beta \end{pmatrix},$$

where  $\beta$  is the root which is given to eight decimal places by  $\beta_0 = 0.67609672 + 0.97831834i$ . Note that the other roots of the polynomial  $\beta^4 + \beta^2 + 2$ , namely  $-\beta_0$  and  $\pm\bar{\beta}_0$ , happen to give representations that are conjugate in  $PSL_2(\mathbb{C})$  either to the above representation or to its complex conjugate, even though this is far from a general phenomenon (Galois conjugates of lattice representations are often non-discrete).

It is easy to see that the single fixed point of  $xy$  is  $-i\beta$ , so that the matrix

$$q = \begin{pmatrix} -i\beta & 0 \\ 1 & 1/\beta^2 \end{pmatrix}$$

conjugates  $xy$  into

$$\begin{pmatrix} 1 & 1 \\ 0 & 1 \end{pmatrix},$$

and then the other generator of the above peripheral subgroup gets conjugated to

$$\begin{pmatrix} -1 & 1 + 2\beta^2 \\ 0 & -1 \end{pmatrix}.$$

Note that

$$(2\beta^2 + 1)^2 = 4\beta^4 + 4\beta^2 + 1 = -7,$$

so that  $1 + 2\beta^2 = \pm i\sqrt{7}$ , and with the above choice of the root  $\beta$  given above, one checks it is actually  $i\sqrt{7}$ . In any case, the cusp section corresponds to a square lattice, generated by 1 and  $i\sqrt{7}$ .

### 2.2.3. m015. Presentation:

$$\langle x, y \mid [x, y^{-1}]x^3[y, x^{-1}]y^2 \rangle$$

#### Generators of a peripheral subgroup:

$$xy, \quad (xy)^2[x, y^{-1}]x[y^{-1}, x]y^{-1}xy$$

#### Shape of the cusp:

$$4(\gamma - 1)$$

#### Triangular generators:

$$yx = \begin{pmatrix} -1 & -\gamma \\ 0 & -1 \end{pmatrix}, \quad xyx = \begin{pmatrix} 1 & 0 \\ \gamma & 1 \end{pmatrix},$$

where  $\gamma$  is a complex root of  $x^3 - x^2 + 1$  (say the one which is approximately  $0.87743883 - 0.74486176i$ ).

The shape of the matrices for the triangular matrices  $yx$  and  $xyx$  is easily guessed from the SnapPy matrices (which gives only numerical approximations of those matrices), and the minimal polynomial for  $\gamma$  is a consequence of the relation given for these generators. Note also that it is clear that  $xy$  and  $xyx$  generate the group.

**2.3. Ford domains in  $H_{\mathbb{R}}^3$ .** The above information allows to study the Ford domains in  $H_{\mathbb{R}}^3$ . The rough idea is to compute a symmetric set of somewhat short words in the generators, to consider their isometric spheres (as well as their images under the cusp group), which gives a “partial” Ford domain (i.e. a polytope that may or may not be equal to the actual Ford domain).

In order to check whether the partial Ford domain is equal to the Ford domain, one can then apply the Poincaré polyhedron theorem in order to check whether copies of the Ford domain under the group tile  $H_{\mathbb{R}}^3$ . The fact that our set of words is symmetric implies that faces of the Ford domain are paired (the face for  $\gamma$  is sent to the one for  $\gamma^{-1}$ ), and one needs to check the cycle conditions (which roughly say that on the level of codimension two faces, the side-pairings induce a local tiling of  $H_R^3$ ).

The Ford domains are by construction invariant under the action of the peripheral subgroups, so they are not fundamental domains (they are only fundamental domains for the decomposition of the group into cosets of a given peripheral subgroup).

The classical way to obtain an actual fundamental domain for the action of the group is to intersect it with a fundamental domain for the action of the cusp group, which is a lattice in  $\mathbb{C}$ . Hence one can simply intersect the Ford domain with a vertical prism over a parallelogram in  $\mathbb{C}$ .

Another way is to select a representative for each orbits of faces of the Ford domain under the action of the cusp group (we may assume that the union of the face representatives is connected). A fundamental domain is then obtained again as a vertical prism, but over a union faces contained in spheres.

Looking at the picture from infinity, we see polygons in  $\mathbb{C}$ , which are depicted in Figure 1 for the three groups that appear in this paper.

The picture for `m004` is very classical, and appears already in [26]. In that case all isometric spheres bounding the Ford domain have the same radius, and they can be taken to be given simply by the spheres of radius 1 centered at points in the Eisenstein lattice  $\mathbb{Z}[\omega]$ ,  $\omega = (-1 + i\sqrt{3})/2$ .

In the other two cases, there are three different radii for the isometric spheres that bound the Ford domain. The pictures can of course be obtained directly in SnapPy (using the `cuspid_neighborhood` command).

### 3. EXCEPTIONAL FILLINGS OF CENSUS MANIFOLDS

It is well known that for every complete finite volume hyperbolic manifold  $M$ , all but finitely many Dehn fillings are hyperbolic, see [34], [21], [25]. For simplicity, we assume that  $M$  only has one cusp, and write  $M(p/q)$  for the Dehn filling of slope  $p/q$ .

Here  $p/q$  is a reduced fraction (or possibly infinity), and is supposed to specify the slope of a circle on the boundary torus that is chosen to bound a meridian in the 2-torus that

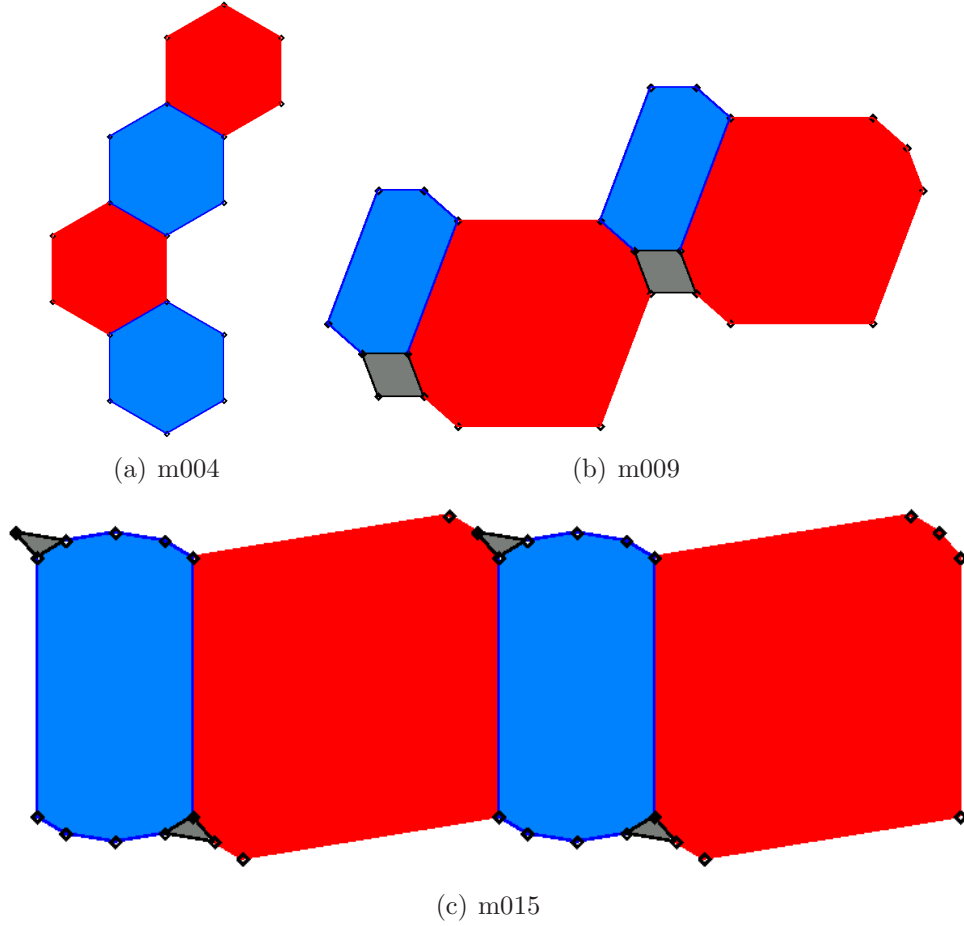


FIGURE 1. Prism description of some 1-cusped hyperbolic manifolds

gets glued to  $M$ . Note that  $M(p/q)$  is only well-defined once a meridian and longitude have been chosen in the boundary torus of  $M$ , which can be done canonically when  $M$  is a knot complement (otherwise we will use the meridian and longitude provided by SnapPy when using the Hildebrand-Weeks census with the notation `m0jk` that we have used throughout the paper).

A lot of work has been done over the years in order to make the “finitely many” part of the statement effective, i.e. to give bounds on the number of all exceptional slopes for knot complements, or to characterize possible Dehn fillings. For instance, exceptional surgeries of 2-bridge knots are classified in [3]. A convenient place to find a list for a lot of manifolds in the beginning of the Hildebrand-Weeks census is [20]. One can also gather a lot of experimental evidence for their statements by using recent versions of SnapPy (simply produce a triangulation for various Dehn-filling, and pass them on to Regina for further analysis).

A key observation, in view of the main statement of [8] (see also Table 1) is that **m004**, **m009** and **m015** all have exceptional Dehn fillings that produce Seifert fibrations over spherical  $(p, q, r)$ -orbifolds (these are often called *small* Seifert fibrations), all with  $p, q, r \geq 3$ . For convenience of notation, we write  $M_4$  (resp.  $M_9$ ,  $M_{15}$ ), for **m004**, **m009** and **m015**.

**Theorem 3.1.** *The following Dehn fillings are small Seifert spaces.*

- $M_4(\pm 3)$  is a Seifert fibration over the  $(3, 3, 4)$ -spherical orbifold.
- $M_9(-2)$  is a Seifert fibration over the  $(3, 3, 5)$ -spherical orbifold.
- $M_{15}(1)$  is a Seifert fibration over the  $(3, 3, 5)$ -spherical orbifold.

These claims can be gathered somewhat painfully from the information in [20], see Proposition 2.2 (26) of that paper. The main difficulty is that the slope of a Dehn filling depends on the basis of the homology that is used. In this paper, we use the basis that is in the SnapPy database, whereas Martelli-Petronio use the basis induced from the canonical bases for the homology of the three boundary components of the magic link complement. The relationship between the two follows from elementary Kirby calculus (see [27], p.265).

Note that Table 8 of [20] also contains the claim about  $M_4 = N(1, 2)$  and  $M_9 = N(1, 3)$  ( $N(p, q)$  denotes a Dehn filling of two of the three cusps of the magic manifold with slopes  $p$  and  $q$  respectively);  $M_9$  is not a knot in  $S^3$ , but it is a knot in  $\mathbb{R}P^3$ .

For the reader who is more versed in geometry than topology, the best way to check Theorem 3.1 is to use SnapPy in conjunction with Regina. Indeed, the following SnapPy commands will produce a triangulation for the Dehn filling of **m009** with slope  $-2$ :

```
M = Manifold('m009')
M.dehn_fill((-2,1))
T = M.filled_triangulation()
T.save()
```

This triangulation can then be imported in Regina; either the manifold is recognized right away, or it can be recognized by performing a Census Lookup (indeed for the Dehn fillings that appear in the present paper, this lookup turns out to be successful). In the above example, Regina describes the Dehn filling by

SFS [S2: (3,1) (3,1) (5,-4)]

where SFS stands for Seifert Fibered Space, and the rest gives gluing information. The base of the fibration is  $S^2$ , and there are three singular fibers, with gluing data given by the following pairs of integers. For the precise meaning of the gluing data, see chapter 12 of [18]. Here we simply mention that the base is a sphere with three orbifold points, with weights 3,3 and 5. In particular, by contracting all the fibers, one gets a homomorphism of  $\pi_1(M_9)$  onto a  $(3, 3, 5)$ -triangle group.

Apart from the possibility of a bug in these well-established computer programs, this computer check can be regarded as a proof because it is purely combinatorial in nature. Note also that we have stated Theorem 3.1 only for motivational purposes. It implies that the fundamental groups of  $M_4$ ,  $M_9$  and  $M_{15}$  all admit homomorphisms onto a  $(3, 3, n)$ -triangle group, with  $n = 4$  or  $5$ ; in fact, in the next section, we will construct explicit such homomorphisms without appealing to Theorem 3.1.

## 4. COMPLEX HYPERBOLIC GEOMETRY AND TRIANGLE GROUPS

The main goal of this section is to give a triangle group interpretation of two of the discrete groups that occur as holonomy groups in the FKR census, namely  $\rho_{4,3}(\pi_1(M_9))$  and  $\rho_{3,3}(\pi_1(M_{15}))$ , see Theorem 4.2. This identification will immediately imply that these holonomy groups are actually conjugate to each other in  $PU(2, 1)$ .

For basics on complex hyperbolic geometry and triangle groups, see [16], [29], [8] for instance. Recall that complex hyperbolic triangle groups generated by three complex involutions  $I_1, I_2, I_3$  that satisfy

$$(I_1 I_2)^p = (I_2 I_3)^q = (I_3 I_1)^r = Id.$$

In that context, the condition  $p, q, r \geq 3$  can be thought of as requiring that the triangle does not have any right angle, or equivalently that the corresponding  $\mathbb{R}$ -Fuchsian triangle group admit non-trivial deformations:

**Proposition 4.1.**  *$(2, q, r)$ -triangle groups in  $PU(2, 1)$  are rigid, but  $(p, q, r)$ -triangle groups with  $p, q, r \geq 3$  have a 1-dimensional character variety.*

**Proof:** This follows from the explicit parametrization of triangle groups. Given an irreducible triangle (i.e. without any global fixed point), we can take three polar vectors  $v_1, v_2, v_3$  to the mirrors of generating involutions as a basis of  $\mathbb{C}^3$ . After suitably normalizing these vectors, we may assume  $\langle v_j, v_j \rangle = 1$  for all  $j$ , and we may also assume  $\langle v_1, v_2 \rangle$  and  $\langle v_2, v_3 \rangle$  are real (but in general,  $\langle v_1, v_2 \rangle$  will not be real). An invariant of the phase change for the  $v_j$ 's is given by the triple Hermitian product

$$\langle v_1, v_2 \rangle \langle v_2, v_3 \rangle \langle v_3, v_1 \rangle,$$

whose argument is sometimes called the angular invariant of the triangle; one checks that for every  $(p, q, r)$ , only an interval of values of the angular invariant can be realized by complex hyperbolic triangles, characterized by requiring that the Hermitian matrix

$$(1) \quad H = \begin{pmatrix} 1 & -\cos \frac{\pi}{r} & -\cos \frac{\pi}{q} \varphi \\ -\cos \frac{\pi}{r} & 1 & -\cos \frac{\pi}{p} \\ -\cos \frac{\pi}{q} \overline{\varphi} & -\cos \frac{\pi}{p} & 1 \end{pmatrix},$$

have negative determinant, where  $\varphi = e^{it}$  and  $t \in \mathbb{R}$  is the angular invariant. Note that  $t = 0$  corresponds to  $\mathbb{R}$ -Fuchsian groups.

When none of the cosines is zero, the signature condition translates to a lower bound on  $\cos t$ , which gives an interval containing 0 of admissible values of  $t$ . If one of the cosines is 0, then all  $(p, q, r)$ -triangle groups are  $\mathbb{R}$ -Fuchsian, and they are all isometric to each other.  $\square$

The following result is a strengthening of the claim that the discrete representations of  $M_9$  and  $M_{15}$  in the FKR census are conjugate. The idea is to identify the image of these representations as explicit triangle groups; the fact that these two 3-manifolds both admit an exceptional Dehn filling that is a Seifert fibration over a 3,3,5-orbifold (see Theorem 3.1)

immediately implies that their fundamental group admits a homomorphism onto the  $3,3,5$ -triangle group (obtained by contracting of the fibers).

In Theorem 4.2, we describe an explicit such homomorphism and show that the corresponding peripheral holonomy is cyclic unipotent; hence the corresponding representations must actually appear somewhere in the FKR census, and they are easily identified in the census list using the field of cross ratios.

**Theorem 4.2.** (1) *Up to conjugacy and complex conjugation, there is a unique  $(3,3,4)$ -triangle group such that  $I_2I_3I_1I_3$  is parabolic. Its even length words subgroup is conjugate to both  $\rho_{1,1}(\pi_1(M_4))$  and  $\rho_{4,1}(\pi_1(M_4))$ , or in other words to the holonomy group of the unique boundary unipotent spherical CR uniformization of the figure eight knot complement.*

(2) *Up to conjugacy and complex conjugation, there is a unique  $(3,3,5)$ -triangle group such that  $I_2I_3I_1I_3$  is parabolic. The even length subgroup of that triangle group is conjugate to both  $\rho_{4,3}(\pi_1(M_9))$  and  $\rho_{3,3}(\pi_1(M_{15}))$ .*

*Remark 4.3.* The triangle groups that appear in Theorem 4.2 are often denoted  $(3,3,4;\infty)$  and  $(3,3,5;\infty)$ , respectively.

**Proof:** We treat the case of  $(3,3,5)$ -triangles, the other one being entirely similar. In that case, the matrix of equation (1) reads

$$(2) \quad H = \begin{pmatrix} 1 & -\frac{1}{2} & -\frac{1+\sqrt{5}}{4}\varphi \\ -\frac{1}{2} & 1 & -\frac{1}{2} \\ -\frac{1+\sqrt{5}}{4}\bar{\varphi} & -\frac{1}{2} & 1 \end{pmatrix},$$

which has negative determinant for  $\varphi = e^{it}$  and  $|t| < \arccos \frac{\sqrt{5}-3}{2}$ .

It is not difficult to verify that 1 is always an eigenvalue of  $I_2I_3I_1I_3$ , and that it has real trace (the latter follows from the fact that it is the product of two involutions, namely  $I_2$  and  $I_3I_1I_3$ , so it is conjugate to its own inverse). In particular, if it is parabolic, then it must actually be unipotent, hence its trace must be equal to 3.

Now even when  $I_2I_3I_1I_3$  is not parabolic, its two other eigenvalues are complex conjugate (provided we work with matrices in  $SU(2,1)$ ), and their sum is

$$\frac{1+\sqrt{5}}{2}(2c+1),$$

which is equal to 2 for  $c = \sqrt{5}/2 - 1$ . This corresponds to taking

$$\varphi = (\sqrt{5} - 2 + i\sqrt{4\sqrt{5} - 5})/2.$$

which is one of the complex roots of the polynomial  $x^4 + 4x^3 + x^2 + 4x + 1$ . In other words, the relevant triangle group can be written in terms of matrices with entries in  $K = \mathbb{Q}(\varphi)$ , which is number field of degree 4 (beware that this extension is not Galois). The matrices actually have entries in the ring of integers  $\mathcal{O}_K$  (recall that generators are complex reflections of order 2).

Note that the above value of  $\varphi$  is indeed in the range where the Hermitian form has signature  $(2, 1)$ . In fact, for that value of  $c$ , one gets

$$\det(H) = -\frac{1 + \sqrt{5}}{16}.$$

### The case of m009

From SnapPy, we gather that  $\pi_1(M_9)$  has the presentation

$$\langle a, b, c, d \mid bac = db, c = ad, ca^{-1}bd^{-1} = id \rangle,$$

with a peripheral subgroup generated by  $b^{-1}adc^{-1}d$  and  $d^{-1}cd^{-1}bc^{-1}db^{-1}$ . This can be simplified to

$$\langle a, d \mid a^2[a, d][a, d^{-1}] \rangle,$$

with a peripheral subgroup generated by  $[d^{-1}, a]d$  and  $d^{-1}a[a, d^{-1}]a^{-1}$ .

We describe an explicit homomorphism from  $\pi_1(M_9)$  to the  $(3, 3, 5)$  triangle group, which maps into the index two subgroup of even length words.

$$\langle I_1, I_2, I_3 \mid (I_1I_2)^3, (I_2I_3)^3, (I_3I_1)^5 \rangle.$$

Hoping that no confusion will arise, we use word notation, so that we write 123212 for  $I_1I_2I_3I_2I_1I_2$ , for instance.

The map

$$\begin{cases} a \mapsto 2132 \\ d \mapsto 1232 \end{cases}$$

extends to a homomorphism  $\sigma : \pi_1(M_9) \rightarrow \Gamma(3, 3, 5; \infty)$ . We skip the routine verification of this statement. Note that, under this homomorphism, it is routine as well to verify that the peripheral subgroups get mapped to cyclic groups generated by a single unipotent element. Specifically, one checks that  $[d^{-1}, a]d$  gets mapped to 2313, whereas  $d^{-1}a[a, d^{-1}]a^{-1}$  gets mapped to  $(2313)^2$ , so that our representation has cyclic unipotent boundary holonomy.

### The case of m015

We now sketch the corresponding arguments for  $\pi_1(M_{15})$ . The geometric presentation from SnapPy has the form

$$\langle a, b, c, d \mid bad, cb^{-1}abd^{-1}, cdc^{-1}a \rangle,$$

which can easily be simplified to

$$\langle a, b \mid b = ab^2a^{-1}[b^{-2}, a^{-1}] \rangle.$$

SnapPy also gives generators for a peripheral subgroup, namely  $d^{-1}c = b^{-1}a^{-1}b$  and  $b^{-1}acbd^{-1}a^{-1}d = b^{-3}a^{-1}b^3a^{-1}b^{-1}$ .

One checks that

$$\begin{cases} a \mapsto 2313 \\ b \mapsto 1313 \end{cases}$$

induces a well-defined homomorphism, and it maps the above two peripheral elements to 131(2313)131 and its inverse, respectively.



Now the homomorphisms we just constructed are both boundary unipotent, these representations must appear somewhere in the FKR census. Up to complex conjugation, there are three representations of  $\pi_1(M_9)$  in the census. The field generated by the cross ratios of the corresponding tetrahedra are different, only one has degree 4, namely that for  $\rho_{4,3}$ . Similarly, there is only one representation of  $\pi_1(M_{15})$  with the same field of cross ratios, namely  $\rho_{3,3}$ .  $\square$

## 5. THE COMPLEX HYPERBOLIC FORD DOMAIN

The Ford domain for boundary unipotent spherical CR uniformization of the figure eight knot complement is studied in [7]. We now sketch the corresponding analog for the manifold  $\mathfrak{m}009$  (giving all details would be much longer than for the figure eight knot complement, but in fact it is not more difficult).

We quickly review some basic material about Ford domains. It is convenient to work with coordinates where the Hermitian form is given by

$$(3) \quad J = \begin{pmatrix} 0 & 0 & 1 \\ 0 & 1 & 0 \\ 1 & 0 & 0 \end{pmatrix},$$

and we write  $p_\infty$  for  $(0, 0, 1)$ . Recall that  $\partial_\infty H_{\mathbb{C}}^2 \setminus \{p_\infty\}$  identifies with the Heisenberg group  $\mathbb{C} \times \mathbb{R}$ , see section 4.2.2 of [16]. This identification is obtained by considering the unipotent stabilizer of  $p_\infty$ ; note that a lower triangular matrix with unit diagonal is an isometry of  $J$  if and only if it has the form

$$M(z, t) = \begin{pmatrix} 1 & 0 & 0 \\ z & 1 & 0 \\ -|z|^2/2 + it & -\bar{z} & 1 \end{pmatrix},$$

for some  $z \in \mathbb{C}$  and  $t \in \mathbb{R}$ . The group of such matrices acts simply transitively on  $\partial_\infty H_{\mathbb{C}}^2 \setminus \{p_\infty\}$ , which gives the identification. One easily computes that

$$M(z, t)M(w, u) = M(z + w, t + u + \operatorname{Im}(z\bar{w})),$$

which suggests a group law on  $\mathbb{C} \times \mathbb{R}$ ; up to a coefficient of 2, this is the Heisenberg group law used in [16], so we call  $(z, t)$  Heisenberg coordinates.

For a subgroup  $\Gamma \subset PU(2, 1)$ , the Ford domain  $F_{\Gamma, p_\infty}$  centered at  $p_\infty$  is given in homogeneous coordinates by the set of vectors  $Z \in \mathbb{C}^3$  that satisfy

$$|\langle P_\infty, Z \rangle| \leq |\langle \tilde{g}P_\infty, Z \rangle|$$

for all  $g \in \Gamma$ , where  $\tilde{g}$  denotes any matrix representative of  $g \in \Gamma$ . For each  $g \in \Gamma$  not fixing  $p_\infty$ , the set of points satisfying

$$(4) \quad |\langle P_\infty, Z \rangle| = |\langle \tilde{g}P_\infty, Z \rangle|$$

is a so-called *bisector*, which we denote by  $\mathcal{B}_g$ . It is a basic fact that the trace at infinity of any such bisector, seen in Heisenberg coordinates, is a *bounded* topological sphere, called a *spinal sphere*.

**Definition 5.1.** *The 3-dimensional polyhedron given by the intersection of the Ford domain  $F_{\Gamma, p_\infty}$  with  $\mathcal{B}_g$  will be denoted by  $b_g$ .*

When  $\Gamma$  is discrete and  $p_\infty$  is not fixed by any non-trivial element in  $\Gamma$ , the Ford domain is actually a fundamental domain for the action of  $\Gamma$ . If  $p_\infty$  has a discrete stabilizer  $P \subset \Gamma$ , then the Ford domain is only a fundamental domain for the decomposition of  $\Gamma$  into  $P$ -cosets (see [9] or [8] for instance).

It is usually difficult to determine this set explicitly, even though it is fairly accessible to experimentation. Indeed, the boundary of this domain is made up of pieces of bisectors, and bisector intersections are now fairly well understood, see [16] for instance. The basic point is that pairs of bisectors that occur in a Ford domain have connected intersection, diffeomorphic to a smooth disk. This important fact is stated in Theorem 9.2.6 of [16] (in Goldman's language, pairs of bisectors that contain faces of a Ford domain are called *covertical* bisectors).

If  $\Gamma$  can be represented by matrices in a given number field (of reasonably small degree), there are computational tools to certify the combinatorics of 2-faces of the Ford domain (see [7]).

We now apply these general notions to the groups that are the images of the relevant FKR representations. Recall that we gave a detailed description of these representations in section 4; our description relied on a specific Hermitian form, see equation (1). In those coordinates, one can easily work out formulas for the matrices  $I_1, I_2, I_3$ , namely

$$I_1 = \begin{pmatrix} 1 & -1 & \alpha \\ 0 & -1 & 0 \\ 0 & 0 & -1 \end{pmatrix}, \quad I_2 = \begin{pmatrix} -1 & 0 & 0 \\ -1 & 1 & -1 \\ 0 & 0 & -1 \end{pmatrix}, \quad I_3 = \begin{pmatrix} -1 & 0 & 0 \\ 0 & -1 & 0 \\ \bar{\alpha} & -1 & 1 \end{pmatrix},$$

where  $\alpha = -1 + (1 + \sqrt{5})(1 - is)/4$  and  $s = \sqrt{4\sqrt{5} - 5}$ .

We start by conjugating these three matrices so that they preserve the standard Hermitian  $J$ , see equation (3), and so that  $I_2 I_3 I_1 I_3$  becomes (lower) triangular. This is done by an easy linear algebra computation, we give one explicit possible conjugation, namely

$$Q = \begin{pmatrix} \sqrt{2} + (3 - \sqrt{5})(-5 + is)/4\sqrt{2} & 0 & -\sqrt{2} + (1 + \sqrt{5})(1 - is)/4\sqrt{2} \\ (2 + (2 - \sqrt{5})(-3 + is))/4\sqrt{2} & \sqrt{2}/2 & -\sqrt{2} \\ (1 - \sqrt{5})(-1 + is)/4\sqrt{2} & 0 & -\sqrt{2} + (1 + \sqrt{5})(-1 + is)/4\sqrt{2} \end{pmatrix}.$$

One easily checks that  $Q^* H Q = J$ . Writing  $\tilde{I}_k = Q^{-1} I_k Q$ , one checks that

$$\tilde{I}_2 = \begin{pmatrix} -1 & 0 & 0 \\ 0 & 1 & 0 \\ 0 & 0 & -1 \end{pmatrix}, \quad \tilde{I}_2 \tilde{I}_3 \tilde{I}_1 \tilde{I}_3 = \begin{pmatrix} 1 & 0 & 0 \\ 1 & 1 & 0 \\ -\frac{1}{2} & -1 & 1 \end{pmatrix}.$$

The matrices for  $\tilde{I}_1$  and  $\tilde{I}_3$  are much more complicated, so we do not write them out. In what follows, we simply will write  $I_k$  for  $\tilde{I}_k$ , since no confusion should arise.

**Definition 5.2.** *Let  $\Gamma$  be the even length subgroup of the  $(3, 3, 5; \infty)$ -triangle group, i.e. the subgroup generated by  $I_1 I_2$  and  $I_2 I_3$ . We define  $a = I_2 I_3 I_1 I_3$ , and write  $A$  for  $a^{-1}$ .*

32, 23; 2321, 1232; 12, 21; 232131, 131232; 32131232, 23213123.

TABLE 2. The list of group elements whose orbit points define ten core faces, i.e. representatives of each orbit of faces under the  $a$ -action.

Recall that the fixed point of  $a$  is  $p_\infty = (0, 0, 1)$ . We write  $F = F_\Gamma = F_{\Gamma, p_\infty}$  for the corresponding Ford domain. By construction, it cannot be a fundamental domain for the action of  $\Gamma$ , since it is invariant under the action of the cyclic group generated by  $a$ . It has infinitely many faces, but there are only ten  $a$ -orbits of faces. Representatives of these orbits are given by the faces  $b_g \subset \mathcal{B}_g$  for elements  $g$  in Table 2. Note that we do not give the shortest possible word in Table 2, because we consider only even length words in the triangle group. For instance,  $32(e_3) = 3(e_3)$ ,  $12(e_3) = 1(e_3)$ , etc.

We will number the elements in Table 2 as  $g_1 = 32, g_2 = 23, g_3 = 2321, \dots, g_{10} = 23213123$  (in the same order as listed in the table), and number the images of these under powers of  $a$  by setting for  $j = 1, \dots, 10$  and  $k \in \mathbb{N}$ ,

$$(5) \quad a^k g_j = g_{10(2k-1)+j}; \quad a^{-k} g_j = g_{20k+j}.$$

The corresponding ten polytopes  $b_{g_1}, \dots, b_{g_{10}}$  are depicted in Figures 2 and 3. The pictures were obtained by parametrizing the 1-skeleton, and mapping the 1-skeleton by a transformation that identifies the ambient bisector with the unit ball in  $\mathbb{R}^3$ , in such a way that the  $\mathbb{C}$ -slices are given by horizontal disks, and  $\mathbb{R}$ -slices are given by vertical lines containing the  $z$ -axis. For an explanation of how this can be done explicitly, see [8] for instance.

A priori, it is not clear why each face should have only finitely many neighboring faces; this follows easily from the fact that the action of  $a$  in the  $x$ -coordinate is a translation, and the fact that the spinal spheres in a Ford domain are given in Heisenberg coordinates by bounded sets (note that if two spinal spheres are disjoint, then the corresponding bisectors are disjoint).

In what follows, we write  $F$  for  $F_{\Gamma, p_\infty}$ , and  $E$  for  $\partial_\infty F \setminus \{p_\infty\} \subset \mathbb{C} \times \mathbb{R}$ . We use Heisenberg coordinates  $(x, y, t)$ , where  $z = x + iy$ . One easily computes the action of  $a = I_2 I_3 I_1 I_3$  to be given by

$$(6) \quad (z, t) \mapsto (z + 1, t - \operatorname{Im}(z)).$$

In particular, this map preserves every horizontal line in the plane  $\operatorname{Im}(z) = 0$ . Each of these lines is a  $\mathbb{R}$ -circle (going through the point  $p_\infty$ ), i.e. it bounds a totally geodesic copies of  $H_{\mathbb{R}}^2$  in  $H_{\mathbb{C}}^2$ . The union of these real planes is the *invariant fan* of  $a$ , see [17].

For the sake of brevity, we write  $p$  rather than  $p_\infty$ .

**Theorem 5.3.** (1) *The maps  $g_k$  define side pairings of  $F$ . More precisely, if  $k$  is odd,  $g_k(b_k) = b_{k+1}$  and  $F \cap g_k(F) = b_{k+1}$ ; when  $k$  is even,  $g_k(b_k) = b_{k-1}$  and  $F \cap g_k(F) = b_{k-1}$ .*  
 (2) *These pairings satisfies the hypotheses of the Poincaré polyhedron theorem for cosets of the unipotent cyclic group  $\langle a \rangle$ .*

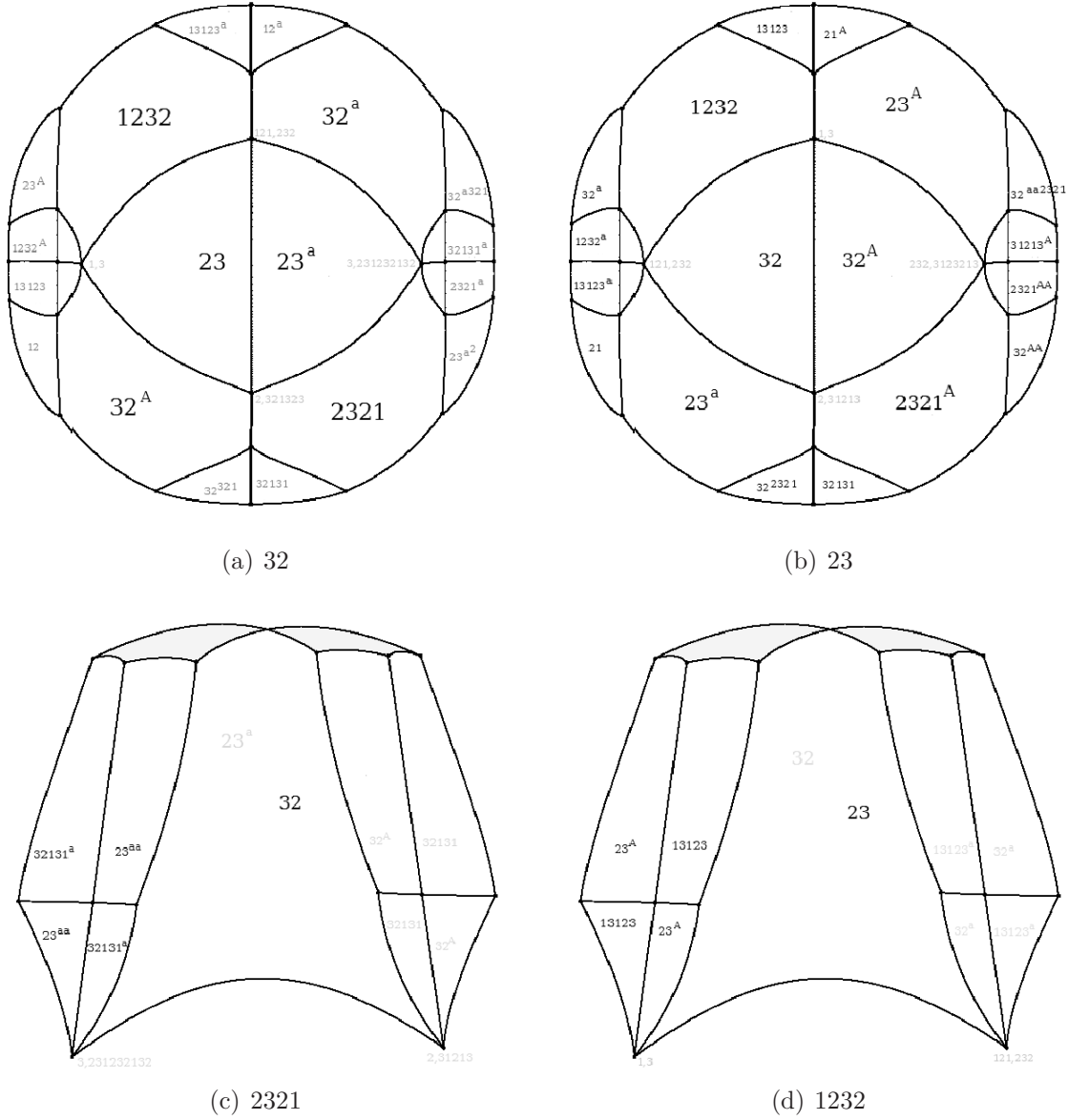


FIGURE 2. Combinatorics of some faces of the Ford domain. In the faces for 23 and 32, there is an extra 16-gon that lies on the boundary at infinity, not drawn in the picture. For other faces, the boundary 2-face is shaded in gray. The Ford domain has infinitely many faces, but every face is the image of one of the depicted 10 faces under an appropriate power of  $a = 2313$  (we write  $A = 3132$  for its inverse); see also Figure 3.

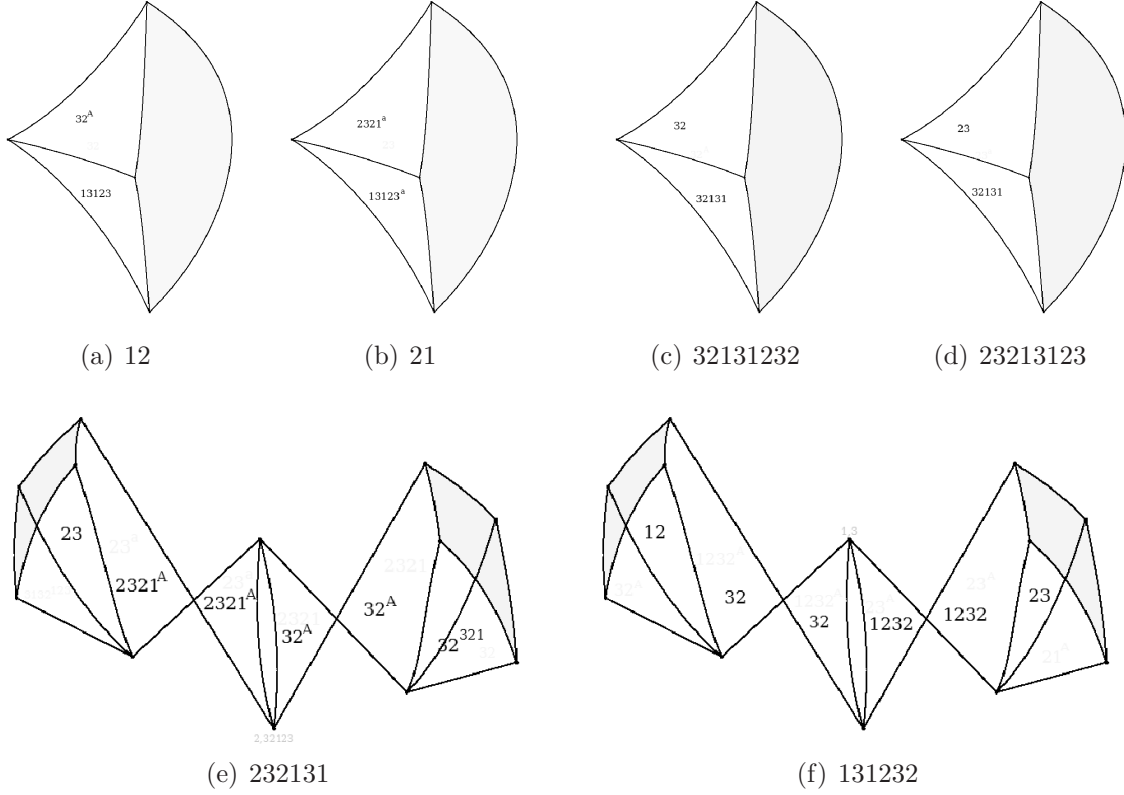


FIGURE 3. More faces of the Ford domain.

(3) *The group  $\Gamma$  has the following presentation,*

$$\langle x_1, x_2 | x_1^3, x_2^3, (x_1 x_2)^5 \rangle,$$

*where we have written  $x_1 = I_1 I_2$ ,  $x_2 = I_2 I_3$ .*

**Proof:** (1) The key for checking this is to certify that the combinatorics given in Figures 2 and 3 are correct. We do not expand on the details, but this can be done because the entries of the generators, as well as the center of the Ford domain, can be given by entries a number field of small degree (here the degree is 4, see page 14).

One easily verifies that the isometries given in Table 2 define side pairings of the Ford domain, by computing several orbits under appropriate group elements. Clearly it is enough to work on the core faces, i.e. the representatives given in Table 2. We will give some detail only for the first two faces, the other ones being entirely similar.

For instance, the fact that  $I_2 I_3$  maps  $b_1$  to  $b_2$  follows from the fact that  $I_2 I_3$  does what is announced in Table 3, where we use the numbering of equation 5. Clearly by construction  $I_2 I_3(B_1) = B_2$ , because  $g_2 = g_1^{-1}$ . The first column of the table means that  $I_2 I_3(B_1 \cap B_2) = B_1 \cap B_2$ , and this follows readily from the fact that  $I_1 I_2$  has order 3.

Point	#2	#3	#4	#5	#7	#8	#9	#11	#12
Image	#1	#22	#12	#11	# 26	# 14	#8	#23	#21
Point	#13	#15	#17	#18	#19	#21	#22	#24	#32
Image	#27	#7	#43	#10	#41	# 4	#6	#18	#30

TABLE 3. Table of correspondence of the 2-faces of  $b_1$  and  $b_2$ , under the natural side pairing map  $I_2I_3 : B_1 \rightarrow B_2$ .

The next column in the table says that  $I_2I_3(B_1 \cap B_3) = B_2 \cap B_{22}$ ; this follows from the fact that

$$I_2I_3(g_3p) = g_{22}p = a^{-1}g_2p.$$

Equivalently, we claim

$$23 \cdot 2321p = 3132 \cdot 23p.$$

This is an obvious consequence of the fact that  $(23)^3 = id$ .

In fact all other claims in the table are all consequences of the relations  $(12)^3$ ,  $(23)^3$  and  $(31)^5$ , as well as the fact that  $2313$  fixes  $p$ . In any event, it should be clear that the claims in the table can readily be checked with a computer (at worst, one performs computation in the relevant number field).

(2) The second item is checked by tracing the Poincaré cycles. Recall that a *ridge* is by definition a codimension two facet of  $F$ . Note that no ridge of the Ford domain is totally geodesic (this requires a computation, it amounts to saying that for  $k \neq l$ ,  $p$ ,  $g_kp$  and  $g_lp$  are never in a common complex line, or in other words, any choice of homogeneous coordinates for these three vectors produces a basis of  $\mathbb{C}^3$ ). By the discussion on page 18, only finitely many checks need to be made, since for  $m$  large enough,  $B_k \cap a^m B_l = \emptyset$ .

The ridges of  $F$  are so-called Giraud disks, which are generic intersections of two bisectors; because the complex spines all intersect in  $p$ , we can think of the intersections as being coequidistant, and in particular their intersections are all smooth disks, equidistant of three points  $p, g_kp, g_lp$ , with  $k \neq l$ .

Because of Giraud's theorem (see [14], [16], [6]), the ridges of  $F$  are on precisely three bisectors, so the local tiling condition near generic ridges is actually a consequence of the existence of side-pairings.

(3) The explicit cycles are obtained by computing orbits of these triples of points under the side pairings; whenever a ridge in the cycle differs from the starting ridge by a power of  $a$ , we close the cycle up by that power of  $a$  (see [9] or [23]).

We work out a few cycles, the other ones being similar. The ridge  $b_1 \cap b_2$  is sent to itself by  $I_2I_3$ , in fact

$$p \xrightarrow{23} 23(p) \xrightarrow{23} 2323(p) = 32(p) \xrightarrow{23} p.$$

This clearly gives a cycle transformation of order 3 preserving that ridge, so we get the relation

$$(23)^3 = id.$$

The ridge  $b_1 \cap b_3$  is slightly more interesting. One checks (most conveniently with a computer), that

$$p, g_1p, g_3p \xleftarrow{2313} p, g_{21}p, g_{23}p \xleftarrow{321313} g_{24}p, g_{21}p, p \xleftarrow{313213} g_2p, p, g_{22}p \xleftarrow{23} p, g_1p, g_3p.$$

The corresponding relation is

$$2313 \cdot 321313 \cdot 313213 \cdot 23 = id,$$

which can be simplified, using  $232 = 323$ , to

$$(12)^3 = id.$$

One easily checks that  $b_1 \cap b_7$  gives

$$(13)^5 = id.$$

Using the relations  $(12)^3 = (23)^3 = (31)^5 = id$ , one checks that the other cycle relations can be reduced to a trivial relation.  $\square$

**Proposition 5.4.** (1) *The only elliptic elements in  $\Gamma$  are conjugates of powers of 12, 23 or 31; in particular, no elliptic element of  $\Gamma$  fixes any point in  $\partial_\infty H_{\mathbb{C}}^2$ .*  
 (2) *The only parabolic elements in  $\Gamma$  are conjugates of powers of 2313.*

**Proof:** (1) As mentioned in the proof of Theorem 5.3, the ridge cycles are all conjugate to powers of 12, 23 or 31. One then considers cycles of lower-dimensional facets, namely 1-faces and vertices.

The cycles of 1-faces turn out to be trivial, and the only non-trivial vertex cycles correspond to the fixed points of 13 and that of 321323 (or conjugates of these under some power of  $a$ ).

(2) Since ideal vertices all have trivial stabilizers, the only parabolic elements in the group are the ones stabilizing the center of the Ford domain, which is by construction a fundamental domain modulo cosets of  $\langle 2313 \rangle$   $\square$

The combinatorial structure of  $\partial E$  can be gathered from the shaded 2-faces in Figures 2 and 3 (apart from the first two faces, where the corresponding boundary 14-gon is not shown on the picture). It may seem somewhat reminiscent of the boundary of the real hyperbolic Ford domain, but it is quite different (unlike the case of the spherical CR uniformization of the figure eight knot complement, see [7]).

Because of the shearing by the imaginary part of  $z$  in formula 6, it is not that easy to produce a meaningful 2-dimensional picture of  $\partial E$ , which is topologically a cylinder. Note that the  $x$ -axis is entirely outside  $E$ , and it gives a core curve for a solid cylinder (in  $\partial_\infty H_{\mathbb{C}}^2$ , one gets a solid torus pinched at  $p_\infty$ ). This means that  $E$  is the complement of a topological solid cylinder; it is in fact a horotube, in Schwartz's terminology [31].

The determination of the topology of the manifold at infinity is somewhat delicate. From the combinatorial description of the  $\partial E$  (together with the action of the cyclic group generated by 2313), one can compute the fundamental group of the manifold. Indeed, one can start with a presentation of the fundamental group of the 1-skeleton, and include a



relation saying that each loop coming from the boundary of a 2-cell becomes trivial in the 2-skeleton.

The bookkeeping of this computation is of course prohibitingly lengthy when performed by hand, but it is fairly well suited to calculations performed by the computer. The end result is that the manifold at infinity does have the same fundamental group as  $m009$ , and one can check the peripheral subgroups are preserved under this isomorphism.

## REFERENCES

- [1] A. F. Beardon. *The Geometry of Discrete Groups*, volume 91 of *Graduate Texts in Mathematics*. Springer-Verlag, New York, 1995.
- [2] N. Bergeron, E. Falbel, and A. Guilloux. Tetrahedra of flags, volume and homology of  $SL(3)$ . To appear in *Geom. Topol.*, arXiv:1101.2742.
- [3] M. Brittenham and Y.-Q. Wu. The classification of exceptional Dehn surgeries on 2-bridge knots. *Comm. Anal. Geom.*, 9(1):97–113, 2001.
- [4] B. Burton. A duplicate pair in the snappea census. arXiv:1311.7615.
- [5] P. Callahan, M. Hildebrand, and J. Weeks. A census of cusped hyperbolic 3-manifolds. *Math. Comp.*, 68(225):321–332, 1999.
- [6] M. Deraux. Deforming the  $\mathbb{R}$ -Fuchsian  $(4,4,4)$ -triangle group into a lattice. *Topology*, 45:989–1020, 2006.
- [7] M. Deraux. A 1-parameter family of spherical CR uniformizations of the figure eight knot complement. Preprint, 2014.
- [8] M. Deraux and E. Falbel. Complex hyperbolic geometry of the figure eight knot. To appear in *Geom. Top.*, arXiv:1303.7096.
- [9] M. Deraux, J. R. Parker, and J. Paupert. New non-arithmetic complex hyperbolic lattices. Preprint, arXiv:1401.0308.
- [10] D. B. A. Epstein and R. C. Penner. Euclidean decompositions of noncompact hyperbolic manifolds. *J. Diff. Geom.*, 27:67–80, 1988.
- [11] E. Falbel. A spherical CR structure on the complement of the figure eight knot with discrete holonomy. *J. Differential Geom.*, 79(1):69–110, 2008.
- [12] E. Falbel, P.-V. Koseleff, and F. Rouillier. Representations of fundamental groups of 3-manifolds into  $PGL(3, \mathbb{C})$ : exact computations in low complexity. Preprint, arXiv:1307.6697.
- [13] E. Falbel and J. Wang. Branched spherical CR structures on the complement of the figure eight knot. Preprint, 2013.
- [14] G. Giraud. Sur certaines fonctions automorphes de deux variables. *Ann. Sci. École Norm. Sup.*, 38:43–164, 1921.
- [15] Garoufalidis S. Goerner M. and Zickert C. Gluing equations for  $PGL(n, \mathbb{C})$ -representations of 3-manifolds. Preprint, arXiv:1207.6711.
- [16] W. M. Goldman. *Complex Hyperbolic Geometry*. Oxford Mathematical Monographs. Oxford University Press, 1999.
- [17] W. M. Goldman and J. R. Parker. Complex hyperbolic triangle groups. *J. Reine Angew. Math.*, 425:71–86, 1992.
- [18] J. Hempel. *3-manifolds*. AMS Chelsea Publishing, Providence, RI, 2004.
- [19] M. Hildebrand and J. Weeks. A computer generated census of cusped hyperbolic 3-manifolds. In *Computers and mathematics (Cambridge, MA, 1989)*, pages 53–59. Springer, New York, 1989.
- [20] B. Martelli and C. Petronio. Dehn filling of the “magic” 3-manifold. *Comm. Anal. Geom.*, 14(5):969–1026, 2006.
- [21] W. Neumann and D. Zagier. Volumes of hyperbolic three-manifolds. *Topology*, 1985:307–332, 24.
- [22] J. R. Parker. Hyperbolic spaces. Jyväskylä lectures in Mathematics, 2008.

- [23] J. R. Parker. *Complex Hyperbolic Kleinian Groups*. Cambridge University Press, To appear.
- [24] J. R. Parker and P. Will. A complex hyperbolic Riley slice. in preparation.
- [25] C. Petronio and J. Porti. Negatively oriented triangulations and a proof of Thurston's hyperbolic Dehn surgery theorem. *Expo. Math.*, 18:16–35, 2000.
- [26] R. Riley. A quadratic parabolic group. *Math. Proc. Cambridge Philos. Soc.*, 77:281–288, 1975.
- [27] D. Rolfsen. *Knots and links*, volume 7 of *Mathematics Lecture Series*. Publish or Perish Inc., Houston, TX, 1990.
- [28] R. E. Schwartz. Degenerating the complex hyperbolic ideal triangle groups. *Acta Math.*, 186(1):105–154, 2001.
- [29] R. E. Schwartz. Complex hyperbolic triangle groups. In *Proceedings of the International Congress of Mathematicians, Vol. II (Beijing, 2002)*, pages 339–349, Beijing, 2002. Higher Ed. Press.
- [30] R. E. Schwartz. Real hyperbolic on the outside, complex hyperbolic on the inside. *Inv. Math.*, 151(2):221–295, 2003.
- [31] R. E. Schwartz. *Spherical CR geometry and Dehn surgery*, volume 165 of *Annals of Mathematics Studies*. Princeton University Press, 2007.
- [32] M. Stover. Volumes of Picard modular surfaces. *Proc. Amer. Math. Soc.*, 139(9):3045–3056, 2011.
- [33] M. Thistlethwaite. Cusped hyperbolic manifolds with 8 tetrahedra. <http://www.math.utk.edu/~morwen/8tet>, 2010.
- [34] W. P. Thurston. The Geometry and Topology of Three-Manifolds. <http://library.msri.org/books/gt3m>, 2002. Princeton lecture notes.